Acta Cryst E CRYSTALLOGRAPHIC COMMUNICATIONS

ISSN 2056-9890

Crystal structure of 2,5-dihydroxyterephthalic acid from powder diffraction data

Joshua D. Vegetabile and James A. Kaduk*

Department of Chemistry, North Central College, 131 S. Loomis, St., Naperville IL, 60540 , USA. *Correspondence e-mail: kaduk@polycrystallography.com

Received 16 September 2022
Accepted 25 September 2022

Edited by W. T. A. Harrison, University of Aberdeen, Scotland

Keywords: powder diffraction; 2,5-dihydroxyterephthalic acid; Rietveld refinement; density functional theory.

CCDC references: 2209514; 2209515; 2209516; 2209517

Supporting information: this article has supporting information at journals.iucr.org/e

The crystal structure of anhydrous 2,5-dhydroxyterephthalic acid, $C_8H_6O_6$, was solved and refined using laboratory X-ray powder diffraction data, and optimized using density functional techniques. The published structure of 2,5-dihydroxyterephthalic acid dihydrate was also optimized. The carboxylic acid groups form strong hydrogen bonds, which form centrosymmetric rings with graph set $R_2^2(8)$. These hydrogen bonds link the molecules into chains along [011]. There is an intramolecular O—H···O hydrogen bond between the hydroxyl group and the carbonyl group of the carboxylic acid. The hydrogen bonding in the dihydrate is very different. Although the intramolecular hydroxy/carboxylic acid hydrogen bond is present, the water molecule acts as an acceptor to the carboxylic acid and a donor to two other oxygen atoms. The carboxylic acid groups do not interact with each other directly.

1. Chemical context

2,5-Dihydroxyterephthalate ($C_8H_4O_6^{2-}$; dhtp) is of current interest as a linker in metal–organic frameworks (MOFs). It can add extra functionality to alter adsorption and catalytic properties. In an attempt to replicate the ionothermal preparation of the Co-dhtp MOF Co_2(dobdc)-ST (Azbell *et al.*, 2022), an unexpected product was obtained, namely anhydrous 2,5-dhydroxyterephthalic acid, $C_8H_6O_6$, (I).

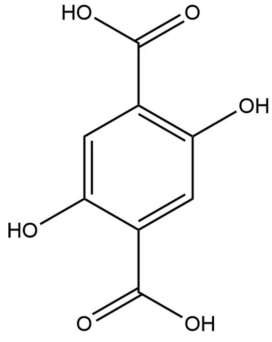

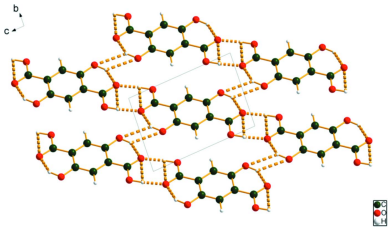

The crystal structures of three Co-dhtp MOFs have been reported: Cambridge Structural Database refcodes FEGBEB (Gen, 2017), VOFJIM (Rosnes *et al.*, 2019) and VOFJIM01 (Ayoub *et al.*, 2019). The calculated powder patterns of these three compounds, which have been given the name CPO-27-Co, indicate that they have the same structure (Fig. 1).

2. Structural commentary

Compound (I) crystallizes in the triclinic space group $P\overline{1}$ with half a molecule in the asymmetric unit. The root-mean-square

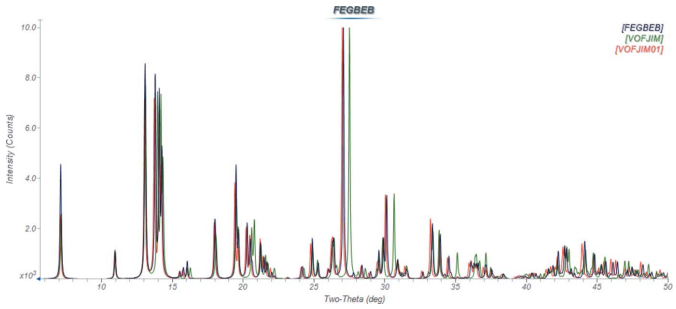

Figure 1
Calculated (using *Mercury;* Macrae *et al.*, 2020) powder diffraction patterns (Cu *Kα* radiation) for CPO-27-Co [FEGBEB (Gen, 2017), VOFJIM (Rosnes *et al.*, 2019) and VOFJIM01 (Ayoub *et al.*, 2019)]. The differences in peak positions result from the different temperatures of the diffraction studies. Image generated using *JADE Pro* (MDI, 2022).

Cartesian displacements of the non-H atoms in the Rietveld-refined and *CRYSTAL17*-optimized structures is 0.053 Å (Fig. 2). The good agreement provides strong evidence that the structure is correct (van de Streek & Neumann, 2014). The *CRYSTAL17* and *VASP*-optimized structures are essentially identical (r.m.s. displacement = 0.031 Å). This discussion concentrates on the *CRYSTAL17*-optimized structure. The full molecule (with atom numbering) is illustrated in Fig. 3 and a view of the packing down the *a*-axis direction is shown in Fig. 4.

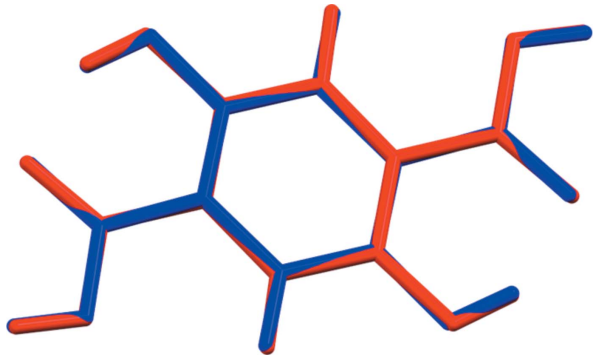

Figure 2
Comparison of the Rietveld-refined (red) and *VASP*-optimized (blue) structures of anhydrous 2,5-dihydroxyterephthalic acid. The r.m.s. Cartesian displacement is 0.053 Å. Image generated using *Mercury* (Macrae *et al.*, 2020).

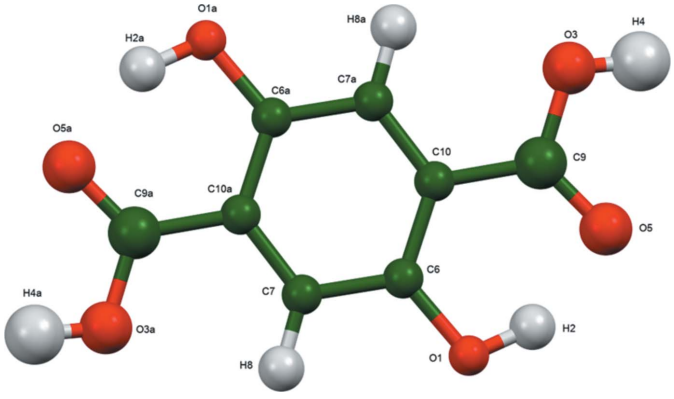

Figure 3
The full 2,5-dihydroxyterephthalic acid molecule, with the atom numbering. The atoms are represented by 50% probability spheroids. Image generated using *Mercury* (Macrae *et al.*, 2020). Symmetry code: (*a*) $1-x, 1-y, 1-z$.

Table 1
Hydrogen-bond geometry (Å, °) for (I).

D—H···A	D—H	H···A	D···A	D—H···A
O3—H4···O5^{i}	1.00	1.69	2.689	174
O1—H2···O5	0.99	1.68	2.567	147

Symmetry code: (i) $-x+1, -y+2, -z+2$.

All of the bond distances, angles, and torsion angles fall within the normal ranges indicated by a *Mercury* Mogul geometry check (Macrae *et al.*, 2020). The plane of the phenyl ring lies approximately on the $(98\bar{9})$ Miller plane. The peak profiles are dominated by anisotropic microstrain broadening: the average microstrain is 8362 ppm.

The Bravais–Friedel–Donnay–Harker (Bravais, 1866; Friedel, 1907; Donnay & Harker, 1937) morphology suggests that we might expect platy (with {001} as the major faces) morphology for this crystal. A 4th order spherical harmonics preferred orientation model was included in the refinement. The refined texture index was 1.059 (2), indicating that preferred orientation was small for this capillary specimen. In flat plate specimens examined in Bragg–Brentano geometry using Cu radiation, the preferred orientation tended to be higher.

3. Supramolecular features

In the extended structure of (I), the carboxylic acid groups form strong O3—H4···O5 hydrogen bonds, which form centrosymmetric loops with graph set $R_2^2(8)$ (Etter, 1990; Bernstein *et al.*, 1995; Shields *et al.*, 2000). These hydrogen bonds link the molecules into chains propagating along [011] (Table 1; Fig. 5). There is an intramolecular O1—H2···O5 hydrogen bond between the hydroxyl group and the carbonyl group of the carboxyl acid. A C—H···O hydrogen bond also contributes to the lattice energy. The *Mercury* aromatics

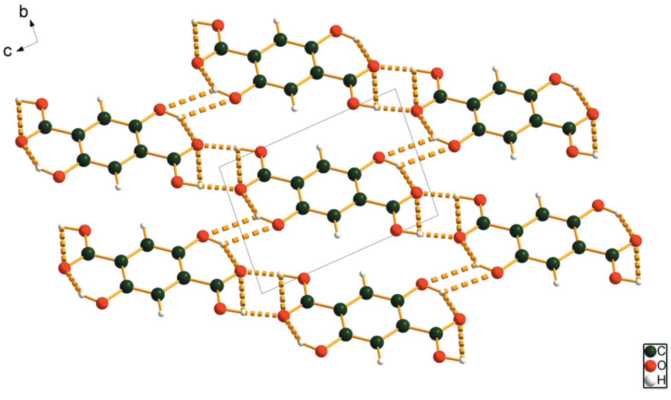

Figure 4
The crystal structure of anhydrous 2,5-dihydroxyterephthalic acid, viewed down the *a*-axis. Image generated using *DIAMOND* (Crystal Impact, 2022).

Table 2
Hydrogen-bond geometry (Å, °) for DUSJUX.

D—H···A	D—H	H···A	D···A	D—H···A
O2—H2···O4	1.07	1.43	2.500	178
O1—H1···O3^{i}	1.01	1.64	2.562	149
O4—H4···O3^{ii}	0.99	1.78	2.736	161
O4—H5···O1^{iii}	0.99	1.82	2.794	169

Symmetry codes: (i) $-x, -y+1, -z+2$; (ii) $x, -y+\frac{3}{2}, z-\frac{1}{2}$; (iii) $-x+1, -y+1, -z+1$.

analyser indicates one strong interaction with a centroid–centroid distance of 4.26 Å, and a moderate one at 5.59 Å.

The hydrogen bonding in the dihydrate DUSJUX (Cheng *et al.*, 2010) is very different (Table 2; Fig. 6). Although the intramolecular hydroxy–carboxylic acid O—H···O hydrogen bond is present, the water molecule acts as an acceptor to the carboxylic acid and a donor to two other oxygen atoms. The carboxylic acid groups do not interact with each other directly.

The *CRYSTAL17* (Dovesi *et al.*, 2018) calculations suggest that DUSJUX is 28.5 kcal mol^{-1} lower in energy than the sum of anhdyrous 2,5-dihydroxyterephthalic acid and two water molecules. The corresponding *VASP* (Kresse & Furthmüller, 1996) calculations indicate that DUSJUX is 114.0 kcal mol^{-1} more stable. As chemists, we would like to attribute the 'extra' energy to the formation of additional hydrogen bonds. Rammohan & Kaduk (2018) developed (for citrates using earlier versions of *CRYSTAL*) a correlation between the energy of an O—H···O hydrogen bond and the Mulliken overlap population between the H and the O acceptor: E (kcal mol^{-1}) = 54.7(overlap)$^{1/2}$. Using this correlation to estimate the energies of the individual hydrogen bonds, we calculate that DUSJUX is 59.6 kcal mol^{-1} lower in energy than the sum of the anhydrous molecule and two water molecules – a value between the two DFT calculations. While the disagreements indicate that the absolute energy calculated for a hydrogen bond may be more uncertain than we would like, the Mulliken overlap population is certainly a guide to whether a hydrogen bond is stronger or weaker than another, and to whether a (geometrically possible) hydrogen bond is real or not.

4. Database survey

A connectivity search in the Cambridge Structural Database [CSD version 5.43 June 2022 (Groom *et al.*, 2016); *ConQuest* 2022.2.0 (Bruno *et al.*, 2002)] of a 2,5-dihydroxyterephthalate fragment with the elements C, H, and O only yielded the

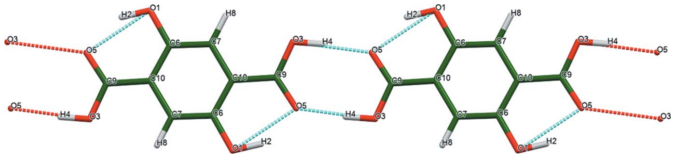

Figure 5
The hydrogen bonds in the structure of anhydrous 2,5-dihydroxyterephthalic acid. Image generated using *Mercury* (Macrae *et al.*, 2020).

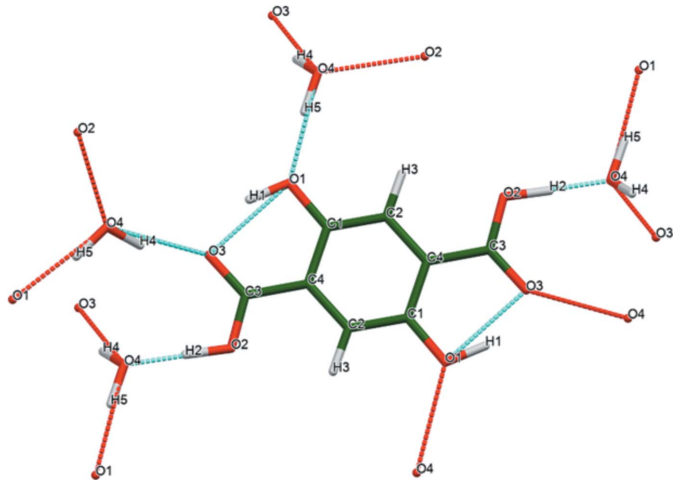

Figure 6
The hydrogen bonds in the structure of 2–5-dihydroxyterephthalic acid dihydrate DUSJUX. Image generated using *Mercury* (Macrae *et al.*, 2020).

structure of the dihydrate (Cheng *et al.*, 2010; DUSJUX), as well as two esters. The dihydrate was also obtained accidentally during the synthesis of metal–organic coordination polymers. Removing the chemistry limitation yielded 249 entries, many of which are metal–organic frameworks. A search of the powder pattern against the Powder Diffraction File (Gates-Rector & Blanton, 2019) yielded no hits. Not even the usual accidental matches were obtained; this pattern evidently occupies a very different portion of 'diffraction space'.

5. Synthesis and crystallization

Cobalt(II) chloride hexahydrate (1.78 g, 7.50 mmol) and 2,5-dihydroxyterephthalic acid (1.00 g, 5.05 mmol) were crushed together with mortar and pestle and added to a 10 ml round-bottom flask. The flask was connected to a Schlenk line and placed in a glass bowl of sand on top of a hot plate. The hot plate was heated to 443 K for approximately 18 h and the round-bottom flask was under vacuum. After being removed from the heat and allowed to cool, the remaining solid was transferred to a Pyrex container with acetonitrile (50 ml) and placed in a vacuum oven at 343 K for 24 h. After removal from the oven, the solution was decanted and replaced with acetonitrile (50 ml). This wash procedure was done a total of three times. The remaining solid was then added to 100 ml of methanol at 343 K for 24 h and decanted, this wash was done two times. The remaining solid was then added to a vacuum oven at 423 K for 24 h. The remaining solid was then added to a scintillation vial wrapped with Parafilm for storage.

6. Refinement

Crystal data, data collection and structure refinement details are summarized in Table 3. A portion of the sample was blended with 11.51% < 1 micron diamond powder (Alfa

Table 3
Experimental details.

	(I)	DUSJUX (DFT)
Crystal data		
Chemical formula	$C_8H_6O_6$	$C_8H_6O_6{\cdot}2(H_2O)$
M_r	198.08	--
Crystal system, space group	Triclinic, $P\overline{1}$	Monoclinic, $P2_1/c$
Temperature (K)	302	--
a, b, c (Å)	4.2947 (5), 5.6089 (5), 8.2331 (19)	5.18830, 17.54500, 5.49900
α, β, γ (°)	93.612 (4), 102.219 (4), 96.7621 (14)	90, 103.03, 90
V (Å^3)	191.69 (1)	487.68
Z	1	2
Radiation type	Mo $K\alpha_{1,2}$, λ = 0.70932, 0.71361 Å	--
Specimen shape, size (mm)	Cylinder, 12 × 0.7	--
Data collection		
Diffractometer	PANalytical Empyrean	
Specimen mounting	Glass capillary	
Data collection mode	Transmission	
Data collection method	Step	
θ values (°)	$2\theta_{min}$ = 1.002 $2\theta_{max}$ = 49.991 $2\theta_{step}$ = 0.008	
Refinement		
R factors and goodness of fit	R_p = 0.034, R_{wp} = 0.042, R_{exp} = 0.019, χ^2 = 5.148	
No. of parameters	53	
No. of restraints	18	
$(\Delta/\sigma)_{max}$	2.635	

The same symmetry and lattice parameters were used for the DFT calculations as for the powder diffraction study for (I). Computer program: *GSAS-II* (Toby & Von Dreele, 2013).

Aesar) internal standard in a mortar and pestle until the color was uniform. The X-ray powder diffraction pattern was measured from a 0.7 mm diameter static capillary specimen on a PANalytical Empyrean diffractometer using Mo $K\alpha$ radiation. The pattern was measured from 1.0–50.0° 2θ in 0.0083560° steps, counting for 4 sec/step.

After correcting the peak positions using the known diamond peak positions, the pattern was indexed using *JADE Pro* (MDI, 2022) on a primitive triclinic cell with a = 4.26420, b = 5.58601, c = 8.17902 Å, α = 93.53, β = 12.13, γ = 96.78° and V = 188 Å^3. Since the volume corresponded to one molecule of 2,5-dihydroxyterephthalic acid, the space group was assumed to be $P\overline{1}$, with half a molecule in the asymmetric unit. A reduced cell search of the CSD yielded no hits. Preliminary indexing attempts using the default peak list from a pattern collected using Cu radiation were unsuccessful (monoclinic cells with no reasonable structures), until closer examination of the pattern revealed that the peak at 21.6° (9.7° Mo) was actually a doublet, and that there was an additional peak at 22.0° (9.9° Mo). Including these two additional peaks yielded the triclinic cell.

The 2,5-dihydroxyterephthalic acid molecule was extracted from the DUSJUX structure using *Materials Studio* (Dassault Systèmes, 2021), and saved as a .mol2 file. The crystal structure was solved using Monte Carlo simulated annealing techniques as implemented in *EXPO2014* (Altomare *et al.*, 2013), using a whole molecule as the fragment. Since the molecule occupies a center of symmetry, the two halves overlapped partially. The overlapping atoms were averaged manually using *Materials Studio* to obtain the asymmetric unit.

Rietveld refinement was carried out using *GSAS-II* (Toby & Von Dreele, 2013). All non-H bond distances and angles were subjected to restraints, based on a *Mercury* Mogul geometry check (Sykes *et al.*, 2011; Bruno *et al.*, 2004). A planar restraint was applied to the benzene ring. The Mogul average and standard deviation for each quantity were used as the restraint parameters. The restraints contributed 1.9% to the final χ^2. The hydrogen atoms were included in calculated positions, which were recalculated during the refinement using *Materials Studio* (Dassault Systèmes, 2021). The U_{iso} of the heavy atoms were grouped by chemical similarity. The U_{iso} for the H atoms were fixed at 1.3× the U_{iso} of the heavy atoms to which they are attached. The peak profiles were described using the generalized microstrain model. The background was modeled using a four-term shifted Chebyshev polynomial, along with a peak at 12.05° to model the scattering from the glass capillary and any amorphous component. The final refinements yielded the residuals reported in Table 1. The largest errors in the

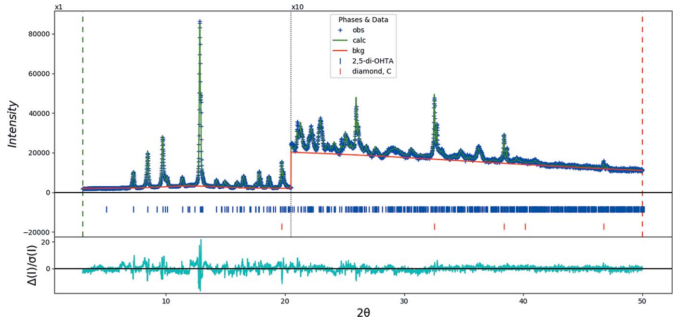

Figure 7
The Rietveld plot for the refinement of anhydrous 2,5-dihydroxyterephthalic acid. The blue crosses represent the observed data points, and the green line is the calculated pattern. The cyan curve is the normalized error plot, and the red line is the background curve. The row of tick marks indicates the calculated reflection positions. The vertical scale has been multiplied by a factor of 10× for $2\theta > 20.5°$. The row of red tick marks indicate the positions of the diamond internal standard peaks.

difference plot (Fig. 7) are small, and are in the shapes of the peaks.

The crystal structure (as well as that of DUSJUX and an isolated water molecule) was optimized using *VASP* (Kresse & Furthmüller, 1996) (fixed experimental unit cells) through the *MedeA* graphical interface (Materials Design, 2016). The calculations were carried out on 16 2.4 GHz processors (each with 4 Gb RAM) of a 64-processor HP Proliant DL580 Generation 7 Linux cluster at North Central College. The calculations used the GGA-PBE functional, a plane wave cutoff energy of 400.0 eV, and a *k*-point spacing of 0.5 $Å^{-1}$ leading to a 4 × 3 × 2 mesh. The structures were also optimized (fixed experimental cells) and population analyses were carried out using *CRYSTAL17* (Dovesi *et al.*, 2018). The basis sets for the H, C, N, and O atoms in the calculations were those of Gatti *et al.* (1994). The calculations were run on a 3.5 GHz PC using 8 *k*-points and the B3LYP functional.

Acknowledgements

We thank Professors Nicholas C. Boaz, Paul F. Brandt and Jeffrey A. Bjorklund for guidance and helpful discusssions.

References

Altomare, A., Cuocci, C., Giacovazzo, C., Moliterni, A., Rizzi, R., Corriero, N. & Falcicchio, A. (2013). *J. Appl. Cryst.* **46**, 1231–1235.
Ayoub, G., Karadeniz, B., Howarth, A. J., Farha, O. K., Đilović, I., Germann, L. S., Dinnebier, R. E., Užarević, K. & Friščić, T. (2019). *Chem. Mater.* **31**, 5494–5501.
Azbell, T., Pitt, T., Bollmeyer, M., Cong, C., Lancaster, K. & Milner, P. (2022). *ChemRxiv*, https://doi.org/10.26434/chemrxiv-2022-00xd7.
Bernstein, J., Davis, R. E., Shimoni, L. & Chang, N. L. (1995). *Angew. Chem. Int. Ed. Engl.* **34**, 1555–1573.
Bravais, A. (1866). *Etudes Cristallographiques*. Paris: Gauthier Villars.
Bruno, I. J., Cole, J. C., Edgington, P. R., Kessler, M., Macrae, C. F., McCabe, P., Pearson, J. & Taylor, R. (2002). *Acta Cryst.* B**58**, 389–397.
Bruno, I. J., Cole, J. C., Kessler, M., Luo, J., Motherwell, W. D. S., Purkis, L. H., Smith, B. R., Taylor, R., Cooper, R. I., Harris, S. E. & Orpen, A. G. (2004). *J. Chem. Inf. Comput. Sci.* **44**, 2133–2144.
Cheng, P.-W., Cheng, C.-F., Chun-Ting, Y. & Lin, C.-H. (2010). *Acta Cryst.* E**66**, o1928.
Crystal Impact (2022). *DIAMOND*. Crystal Impact GbR, Bonn, Germany. https://www.crystalimpact.de/diamond
Dassault Systèmes (2021). *Materials Studio*. BIOVIA, San Diego, USA.
Donnay, J. D. H. & Harker, D. (1937). *Am. Mineral.* **22**, 446–447.
Dovesi, R., Erba, A., Orlando, R., Zicovich–Wilson, C. M., Civalleri, B., Maschio, L., Rérat, M., Casassa, S., Baima, J., Salustro, J. & Kirtman, B. (2018). *WIREs Comput. Mol. Sci.* **8**, e1360.
Etter, M. C. (1990). *Acc. Chem. Res.* **23**, 120–126.
Friedel, G. (1907). *Bull. Soc. Fr. Mineral.* **30**, 326–455.
Gates-Rector, S. & Blanton, T. (2019). *Powder Diffr.* **34**, 352–360.
Gatti, C., Saunders, V. R. & Roetti, C. (1994). *J. Chem. Phys.* **101**, 10686–10696.
Gen, Z. L. (2017). Private communication (refcode FEGBEB). CCDC, Cambridge, England. https://doi.org/10.5517/ccdc.csd.cc1pfslh
Groom, C. R., Bruno, I. J., Lightfoot, M. P. & Ward, S. C. (2016). *Acta Cryst.* B**72**, 171–179.
Kresse, G. & Furthmüller, J. (1996). *Comput. Mater. Sci.* **6**, 15–50.
Macrae, C. F., Sovago, I., Cottrell, S. J., Galek, P. T. A., McCabe, P., Pidcock, E., Platings, M., Shields, G. P., Stevens, J. S., Towler, M. & Wood, P. A. (2020). *J. Appl. Cryst.* **53**, 226–235.
Materials Design (2016). *MedeA*. Materials Design Inc., Angel Fire, NM, USA.
MDI (2022). *JADE Pro*. Materials Data, Livermore, CA, USA.
Rammohan, A. & Kaduk, J. A. (2018). *Acta Cryst.* B**74**, 239–252.
Rosnes, M. H., Mathieson, J. S., Törnroos, K. W., Johnsen, R. E., Cronin, L. & Dietzel, P. D. C. (2019). *Cryst. Growth Des.* **19**, 2089–2096.
Shields, G. P., Raithby, P. R., Allen, F. H. & Motherwell, W. D. S. (2000). *Acta Cryst.* B**56**, 455–465.
Streek, J. van de & Neumann, M. A. (2014). *Acta Cryst.* B**70**, 1020–1032.
Sykes, R. A., McCabe, P., Allen, F. H., Battle, G. M., Bruno, I. J. & Wood, P. A. (2011). *J. Appl. Cryst.* **44**, 882–886.
Toby, B. H. & Von Dreele, R. B. (2013). *J. Appl. Cryst.* **46**, 544–549.

supporting information

Acta Cryst. (2022). E**78**, 1061-1065 [https://doi.org/10.1107/S2056989022009409]

Crystal structure of 2,5-dihydroxyterephthalic acid from powder diffraction data

Joshua D. Vegetabile and James A. Kaduk

Computing details

2,5-Dihydroxybenzene-1,4-dicarboxylic acid (I)

Crystal data

$C_8H_6O_6$
M_r = 198.08
Triclinic, $P\overline{1}$
Hall symbol: -P 1
a = 4.2947 (5) Å
b = 5.6089 (5) Å
c = 8.2331 (19) Å
α = 93.612 (4)°
β = 102.219 (4)°
γ = 96.7621 (14)°
V = 191.69 (1) Å^3
Z = 1
D_x = 1.716 Mg m^{-3}
T = 302 K
cylinder, 12 × 0.7 mm

Data collection

PANalytical Empyrean diffractometer
Specimen mounting: glass capillary
Data collection mode: transmission
Scan method: step

Refinement

18 restraints
Preferred orientation correction: Simple spherical harmonic correction Order = 4 Coefficients: 0:0:C(2,-2) = 0.246(11); 0:0:C(2,-1) = -0.018(11); 0:0:C(2,0) = -0.313(16); 0:0:C(2,1) = 0.217(13); 0:0:C(2,2) = -0.192(9); 0:0:C(4,-4) = -0.146(17); 0:0:C(4,-3) = 0.073(19); 0:0:C(4,-2) = -0.052(16); 0:0:C(4,-1) = 0.083(18); 0:0:C(4,0) = -0.058(17); 0:0:C(4,1) = -0.006(18); 0:0:C(4,2) = -0.196(23); 0:0:C(4,3) = 0.071(16); 0:0:C(4,4) = 0.108(25)

Fractional atomic coordinates and isotropic or equivalent isotropic displacement parameters (Å^2)

	x	*y*	*z*	U_{iso}*/U_{eq}
C10	0.492 (2)	0.6406 (16)	0.6392 (11)	0.0323 (10)*
C6	0.6818 (18)	0.4506 (18)	0.6571 (9)	0.0323 (10)*
C7	0.6946 (18)	0.3106 (14)	0.5107 (12)	0.0323 (10)*
C9	0.477 (2)	0.7892 (16)	0.7918 (9)	0.0553 (15)*
O1	0.8599 (12)	0.4082 (9)	0.8120 (6)	0.0323 (10)*

O3	0.2791 (12)	0.9640 (12)	0.7718 (7)	0.0553 (15)*
O5	0.6452 (16)	0.7744 (11)	0.9376 (9)	0.0553 (15)*
H8	0.84185	0.17135	0.52928	0.0420 (14)*
H2	0.83782	0.54288	0.88998	0.0420 (14)*
H4	0.30280	1.07255	0.87663	0.0719 (19)*

Geometric parameters (Å, º)

C10—C6	1.411 (5)	C9—O3	1.365 (5)
C10—C7^{i}	1.384 (5)	C9—O5	1.277 (5)
C10—C9	1.482 (6)	O1—C6	1.391 (5)
C6—C10	1.411 (5)	O1—H2	0.987 (5)
C6—C7	1.412 (6)	O3—C9	1.365 (5)
C6—O1	1.391 (5)	O3—H4	1.004 (6)
C7—C10^{i}	1.384 (5)	O5—C9	1.277 (5)
C7—C6	1.412 (6)	H8—C7	1.060 (8)
C7—H8	1.060 (8)	H2—O1	0.987 (5)
C9—C10	1.482 (6)	H4—O3	1.004 (6)
C6—C10—C7^{i}	124.3 (7)	C10^{i}—C7—H8	126.7 (10)
C6—C10—C9	118.1 (9)	C6—C7—H8	115.1 (10)
C7^{i}—C10—C9	117.5 (9)	C10—C9—O3	116.8 (7)
C10—C6—C7	117.4 (6)	C10—C9—O5	125.0 (9)
C10—C6—O1	121.6 (9)	O3—C9—O5	118.1 (7)
C7—C6—O1	121.0 (10)	C6—O1—H2	105.5 (6)
C10^{i}—C7—C6	118.1 (7)	C9—O3—H4	112.7 (5)

Symmetry code: (i) −*x*+1, −*y*+1, −*z*+1.

(Ia)

Crystal data

C
M_r = 12.01
Cubic, $Fd\bar{3}m$
Hall symbol: -F 4vw 2vw
a = 3.58625 (11) Å
V = 46.12 (1) Å^3
Z = 8
D_x = 3.459 Mg m^{-3}
T = 302 K

Refinement

Preferred orientation correction: March-Dollase correction coef. = 1.000 axis = [0, 0, 1]

Fractional atomic coordinates and isotropic or equivalent isotropic displacement parameters (Å^2)

	x	*y*	*z*	U_{iso}*/U_{eq}
C1	0.12500	0.12500	0.12500	0.0159*

Geometric parameters (Å, º)

C1—C1^{i}	1.5529	C1—C1^{iii}	1.5529
C1—C1^{ii}	1.5529	C1—C1^{iv}	1.5529

C1^{i}—C1—C1^{ii}	109.471	C1^{i}—C1—C1^{iv}	109.471
C1^{i}—C1—C1^{iii}	109.471	C1^{ii}—C1—C1^{iv}	109.471
C1^{ii}—C1—C1^{iii}	109.471	C1^{iii}—C1—C1^{iv}	109.471

Symmetry codes: (i) x+1/4, y+1/4, −z; (ii) −z, x+1/4, y+1/4; (iii) y+1/4, −z, x+1/4; (iv) −x, −y, −z.

(I_DFT)

Crystal data

$C_8H_6O_6$	c = 8.1976 Å
M_r = 198.08	α = 93.6590°
Triclinic, $P\overline{1}$	β = 102.1730°
a = 4.2647 Å	γ = 96.7840°
b = 5.5912 Å	Z = 1

Data collection

h = →	l = →
k = →	

Fractional atomic coordinates and isotropic or equivalent isotropic displacement parameters (Å^2)

	x	y	z	U_{iso}*/U_{eq}
C10	0.50725	0.65165	0.64068	0.06414*
C6	0.68695	0.46350	0.65571	0.06414*
C7	0.69097	0.31393	0.51546	0.06414*
C9	0.48403	0.80691	0.79069	0.01062*
O1	0.87656	0.42423	0.80458	0.01062*
O3	0.28942	0.97462	0.76830	0.01062*
O5	0.65017	0.78063	0.93109	0.01062*
H8	0.84185	0.17135	0.52928	0.08339*
H2	0.83782	0.54288	0.88999	0.01381*
H4	0.30280	1.07255	0.87663	0.01381*

Bond lengths (Å)

C10—C6	1.370	C7—H8	1.079
C10—C7^{i}	1.415	C9—O3	1.320
C10—C9	1.487	C9—O5	1.245
C6—C7	1.382	O1—H2	0.986
C6—O1	1.361	O3—H4	1.000
C7—C10^{i}	1.415	H4—O3	1.000

Symmetry code: (i) −x+1, −y+1, −z+1.

Hydrogen-bond geometry (Å, º)

D—H···A	D—H	H···A	D···A	D—H···A
O3—H4···O5^{ii}	1.00	1.69	2.689	174
O1—H2···O5	0.99	1.68	2.567	147

Symmetry code: (ii) −x+1, −y+2, −z+2.

(DUSJUX_DFT)

Crystal data

$C_8H_6O_6·2(H_2O)$
Monoclinic, $P2_1/c$
a = 5.18830 Å
b = 17.54500 Å
c = 5.49900 Å
β = 103.03°
V = 487.68 Å^3
Z = 2

Data collection

$h = \rightarrow$
$k = \rightarrow$
$l = \rightarrow$

Fractional atomic coordinates and isotropic or equivalent isotropic displacement parameters (Å^2)

	x	y	z	B_{iso}*/B_{eq}
O1	0.02829	0.35100	0.84164	
H1	−0.08229	0.31915	0.93268	
O2	0.41842	0.59430	0.63866	
H2	0.51266	0.64044	0.56603	
O3	0.28123	0.68492	0.87357	
C1	0.01145	0.42401	0.92007	
C2	0.14692	0.48106	0.82449	
H3	0.26253	0.46707	0.68792	
C3	0.28585	0.61663	0.80175	
C4	0.13841	0.55682	0.90233	
O4	0.64658	0.70011	0.46632	
H4	0.52537	0.74263	0.39890	
H5	0.75145	0.68680	0.34282	

Hydrogen-bond geometry (Å, º)

D—H···A	D—H	H···A	D···A	D—H···A
O2—H2···O4	1.07	1.43	2.500	178
O1—H1···O3^{i}	1.01	1.64	2.562	149
O4—H4···O3^{ii}	0.99	1.78	2.736	161
O4—H5···O1^{iii}	0.99	1.82	2.794	169

Symmetry codes: (i) −x, −y+1, −z+2; (ii) x, −y+3/2, z−1/2; (iii) −x+1, −y+1, −z+1.